Superconductivity-induced effects on phononic and electronic Raman scattering in twin-free $YBa_2Cu_3O_{7-x}$ single crystals

M. F. Limonov,* A. I. Rykov, and S. Tajima
Superconductivity Research Laboratory, International Superconductivity Technology Center, 10-13, Shinonome 1-Chome, Koto-ku, Tokyo 135-0062, Japan

A. Yamanaka
Chitose Institute of Science and Technology, Chitose, Hokkaido 066-8655, Japan
(Received 6 December 1999)

Raman scattering spectra have been investigated in twin-free $YBa_2Cu_3O_{7-x}$ single crystals with various oxygen content. Superconductivity-induced effects are found for all A_g phonons in the overdoped crystals, but they rapidly weaken with reducing oxygen content. The 340 cm^{-1} phonon line is analyzed in detail by means of the Green function, as well as the standard Fano formula. The results provide much evidence for the nodal structure of a superconducting gap. The polarization dependence, which is significant in the highly doped crystals, illustrates the *x-y* anisotropy of the electronic response $\chi(\omega)=-R(\omega)+i\rho(\omega)$ and implies a difference of the superconducting gap amplitudes $\Delta_x \neq \Delta_y$ in the $\mathbf{k}_x$ and $\mathbf{k}_y$ directions in the two-dimensional Brillouin zone for orthorhombic $YBa_2Cu_3O_{7-x}$. The gap energy difference $(\Delta_y-\Delta_x)$ decreases as the doping level is deduced.

I. INTRODUCTION

From the very beginning of the investigation of high-temperature superconductors, phononic Raman scattering has been widely used to study the electronic state and superconductivity mechanism. The phonon anomaly at the superconducting transition T_c has been most intensively studied for $YBa_2Cu_3O_{7-x}$. An important finding by Macfarlaine, Rose, and Seky is the softening of the 340 cm^{-1} mode frequency below T_c.[1] The softening and linewidth broadening of this mode were confirmed by many research groups.[2–5] The other phonon anomalies, hardening of the A_g modes at 430 and 500 cm^{-1} below T_c, were also observed by several groups.[6–8] These superconductivity-induced effects are an indication of a rather strong electron-phonon interaction in this material. Zeyher and Zwicknagl have theoretically studied the phonon self-energy effects at $q=0$, for isotropic *s*-wave superconductors.[9] The Zeyher-Zwicknagl model predicts that the opening of an isotropic gap results in a softening for the phonons with frequencies $\hbar\omega<2\Delta$ without any change in the linewidth, whereas for the phonons with $\hbar\omega>2\Delta$ a hardening with an additional broadening is predicted.

On the other hand, the phonon self-energy effects for the gaps with nodes were theoretically examined by Nicol, Jiang, and Carbotte.[10] The main difference from the *s*-wave case is a broadening of phonons with $\hbar\omega<2\Delta$ below T_c, which originates from a finite density of states (DOS) within the maximum gap energy $2\Delta_{max}$ of an anisotropic gap. When the 2Δ peak of the DOS reaches the phonon energy at a certain temperature $T_g<T_c$, the effect of broadening becomes the strongest, resulting in a maximum linewidth at T_g. In spite of their detailed calculation, there has been no analysis of experimental Raman scattering spectra (RSS) by the approach of a gap with nodes.

Electronic Raman scattering also gives rich information about the electronic response of the system including a superconducting gap. The difference between the B_{1g} and A_{1g} electronic continua in the superconducting state was discussed in terms of the *d*-wave symmetry of a gap,[11] which has demonstrated an advantage of Raman scattering spectroscopy, which is sensitive to the symmetry and can detect a part of the Fermi surface selectively.

In the present study, we have precisely measured the RSS of both phononic and electronic origins in detwinned $YBa_2Cu_3O_{7-x}$ crystals with various oxygen contents and found that an interpretation on the basis of an anisotropic gap is more appropriate than the isotropic *s*-wave scenario. To extract the phonon parameters, we analyzed the spectra on the basis of the Green function, which treats both phonon and electronic systems as well as their interaction. We also examined another approach based on the Fano formula, which has been widely used for extracting phonon parameters from the RSS of high-temperature superconductors. The results of the Fano analysis were in good agreement with those from the Green function approach. The physical meaning of the *x-y* anisotropy appearing in the phonon frequency and linewidth in the case of the Fano free parameters fitting has been made clear.

A difficulty in the analysis of the RSS for $YBa_2Cu_3O_{7-x}$ crystals is due to the orthorhombic symmetry, which introduces a mixing of A_{1g} and B_{1g} components both in the phonon and electronic systems. If the effect of this mixing is very strong, the tetragonal approximation does not hold, though it has been adopted in almost all theoretical studies for this material. The *x-y* anisotropy observed in the RSS of fully oxygenated $YBa_2Cu_3O_7$ crystals in our previous work[12] is a typical example of this A_{1g}-B_{1g} mixing. In this study, we also examine the limitation of the tetragonal approach and address possible interpretations for the observed *x-y* anisotropy and its doping dependence.

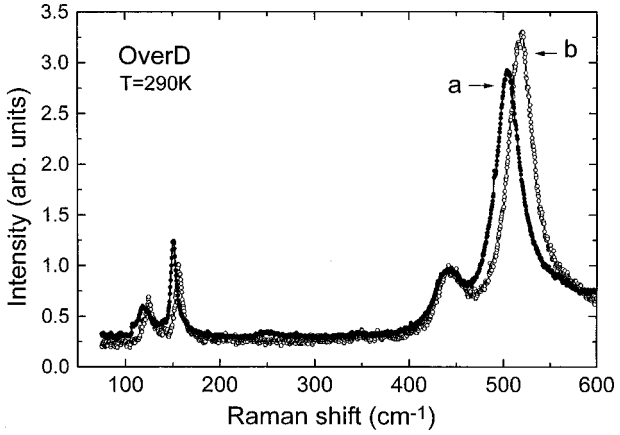

FIG. 1. The Raman spectra of the OverD $YBa_2Cu_3O_{7-x}$ single crystals in the *zz* polarization obtained at room temperature from the lateral *ac* surface before (a) and after (b) polishing.

II. EXPERIMENT

The high-quality $YBa_2Cu_3O_{7-x}$ single crystals were grown by a top-seeded pulling technique and oxygenated under uniaxial pressure in order to obtain the orthorhombic twin-free samples as described previously.[13] The crystals with a typical volume of 10 mm^3 and the highest T_c of 92–93 K with a very narrow transition width $\Delta T_c \leqslant 0.2$ K were post-annealed at 320 °C for higher oxygenation. This post-annealing enhances the in-plane anisotropy and makes the oxygen content close to $\langle\langle O_{7.0}\rangle\rangle$, which results in an overdoped state with lower $T_c = 86$ K and $\Delta T_c = 0.4$ K. In this study, two fully oxygenated samples were prepared from different single crystals and annealed independently. The Raman results for these overdoped (OverD) crystals agree very well. We also studied a series of twin-free $YBa_2Cu_3O_{7-x}$ single crystals with different oxygen contents, namely a slightly overdoped (SlOverD) sample with $T_c = 89$ K, an optimally doped (OptD, $T_c = 93$ K), and the underdoped (UndD, $T_c = 80$ K) crystal.

The RSS were examined by a triple-stage spectrometer with a liquid-nitrogen-cooled charge-coupled device (CCD) detector (T64000 Jobin-Ivon). A typical spectral resolution was 3 cm^{-1}, and several spectra were measured with a resolution of 1 cm^{-1}. For accurate studying of the temperature dependence of RSS and for eliminating a systematical error in the determination of the frequency shifts, RSS were recorded in the spectrograph mode; i.e., the spectral regime was fixed without any scanning of the diffraction gratings. The 514.5 nm line of an Ar-Kr laser was used for the excitation. The power density ranged from 0.2 to 1 W/cm^2 on the sample surface, and consequently the overheating was suppressed down to less than 3 K in all experiments. At low temperatures, a closed-cycle UHV cryostat was used with the temperature stabilization better than 1 K.

The *xx*- and *yy*-polarized RSS were obtained in the pseudobackscattering configuration from the same point on the mirrorlike native regions of crystals by rotating the polarizers. The *zz*-polarized RSS, taken from the *ac* or *bc* surfaces, were essentially the same for both native and cleft surfaces. We have also found that some polishing of the *ac* or *bc* planes with Al_2O_3 abrasive leads to a pronounced reconstruction of the surface. Figure 1 shows the RSS with the

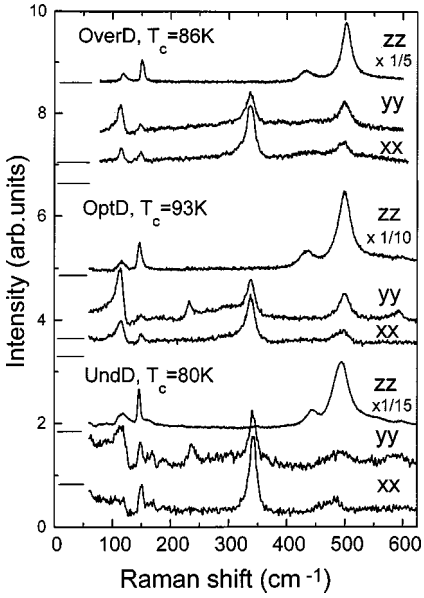

FIG. 2. The Raman spectra of the OverD, OptD, and UndD twin-free $YBa_2Cu_3O_{7-x}$ single crystals in the *xx*, *yy*, and *zz* polarizations at room temperature.

zz polarization, which were obtained from the same *ac* plane before and after polishing. Upon polishing the surface, all four A_g modes shift to the high-frequency side, increase, and their linewidth becomes slightly broadened. This polishing effect cannot be associated with a simple chemical substitution of the native atoms by impurities, because in this case different A_g lines should shift in different directions.[14,15] The effect cannot originate from a disorder in the oxygen sublattice, because no additional Raman line appears in the observed RSS. The most probable explanation is that polishing introduces internal stress in the ac/bc surface. Note that the RSS taken from the *ab* surface do not show any effect of polishing. In order to estimate the values of the internal stress, one can invoke the dependence of Raman frequencies on the hydrostatic pressure $\nu(P)$.[16,17] The pressure coefficients $d\nu/dP$ (cm^{-1}/GPa) were reported to be 1.3 for the 150 cm^{-1} line, 4.4 for the 430 cm^{-1} one, and 5.5 for the 500 cm^{-1} one.[17] The observed shift indicates the existence of an internal pressure of about 3 GPa. In this connection, a similar effect was observed in the polished $RBa_2Cu_3O_{7-x}$ (R = Nd, La, Ho) ceramics. In addition, Raman-forbidden modes were activated by polishing in Ca_2CuO_3, $SrCuO_2$, and La_2CuO_4 ceramics.[18] In this study, all RSS of $YBa_2C_3O_{7-x}$ crystals were obtained from unpolished surfaces.

III. EXPERIMENTAL RESULTS AND ANALYSIS

Figure 2 shows the *xx*-, *yy*-, and *zz*-polarized room-temperature RSS of three twin-free $YBa_2C_3O_{7-x}$ single crystals with different oxygen content, namely, OverD, OptD, and UndD crystals. In all the RSS, five well-known lines with A_g symmetry are clearly seen.[19,20] Hereafter, we refer to these lines as the 120, 150, 340, 430, and 500 cm^{-1} lines. The low-frequency 120 and 150 cm^{-1} lines are ascribed mainly to *z* displacements of heavy atoms, Ba and planar Cu(2), respectively. The 340 cm^{-1} mode belongs to B_{1g} in the tetragonal $YBa_2C_3O_6$ structure (point group D_{4h}) and its

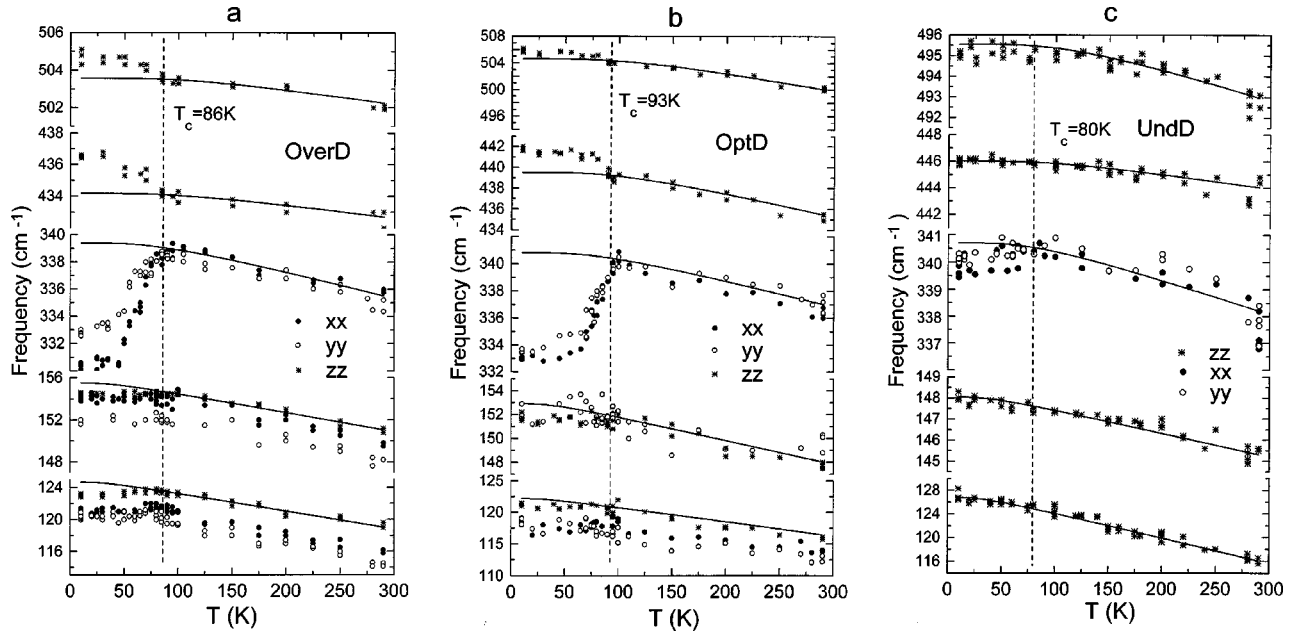

FIG. 3. Temperature dependences of the phonon-line peak frequencies of the five A_g modes for the OverD (a), OptD (b), and UndD (c) twin-free $YBa_2Cu_3O_{7-x}$ single crystals. All lines are the results of calculations within a framework of a two-phonon-decay anharmonicity using Eq. (1).

displacement is the out-of-phase equal amplitude of the O(2) and O(3) oxygens along the *z* direction. In the orthorhombic $YBa_2C_3O_{7-x}$ structure (point group D_{2h}), the symmetry of the 340 cm^{-1} mode is transferred to A_g, and the *z* displacements of the O(2) and O(3) atoms become nonequivalent. However, this mode still has B_{1g} character even in orthorhombic $YBa_2C_3O_{7-x}$, because the deviation from the ideal B_{1g} displacement is expected to be small, less than 10%.[21] The 430 cm^{-1} line is mainly due to in-phase *z* displacements of the O(2) and O(3) oxygens, and the 500 cm^{-1} one is associated with the apical oxygen O(1) displacements along the *z* axis.

For the RSS of OverD crystals (Fig. 2), there are no additional lines caused by structural disorder such as oxygen deficiency. When oxygen content decreases, the *yy*-polarized RSS are rather modified, since oxygen defects are mainly formed in the Cu(1)O(4) chain along the *y* axis. The lines at about 230 and 580–600 cm^{-1} are assigned as the vibrations of Cu(1) and O(4), respectively.

It is worth noting that the observed peak frequencies and linewidths depend strikingly on the polarization configuration. This demonstrates that every nondegenerated A_g peak is renormalized by the interaction with the background electron continuum. For example, the 120 cm^{-1} line shows a pronounced out-of-plane anisotropy of the observed peak frequency, $\Omega_{\max,z} > \Omega_{\max,x}, \Omega_{\max,y}$. Its line shape is quite asymmetric (the Fano-like shape) in the *yy* spectrum, which contains the strongest electronic Raman scattering. On the contrary, the line shape in the *zz* spectrum, where the electronic scattering is very weak, is well described by a Lorentzian.

The temperature dependences of the peak frequencies are plotted in Fig. 3. The normal-state behavior of the frequencies can be described by a simple two-phonon-decay picture:[22]

$$\Omega(T) = \Omega(T_0) - \Omega_0[1 + 2n(\omega/2, T)],$$
$$n(\omega, T) = 1/[\exp(\hbar\omega/k_B T) - 1]. \tag{1}$$

At $T < T_c$, remarkable changes take place in all the phonon lines. For the OverD crystals, softening of the 120, 150, and 340 cm^{-1} modes and hardening of the 430 and 500 cm^{-1} modes demonstrate that the phonon frequencies are renormalized by the redistribution of the electronic continuum in the superconducting state [Fig. 3(a)]. When doping is reduced, the frequency anomaly becomes weak. Among the five phonon lines, the superconductivity-induced anomaly is most robust on the 340 cm^{-1} line presumably because this phonon strongly couples with the electronic system owing to its B_{1g} character.

For a detailed discussion, it is necessary to extract the phonon parameters correctly by a proper fitting procedure. Here we used the method based on the Green function operator.[23] In the case of the tetragonal system, Chen *et al.*[24] proposed the following formula for the electron-phonon coupled Raman spectrum:

$$F(\omega) = AB(\omega)\left\{\rho(\omega) + \frac{1}{\Gamma(1+\varepsilon^2)}\left[\frac{S^2}{V^2} + 2\rho(\omega)\varepsilon S - \rho^2(\omega)V^2\right]\right\}, \tag{2}$$

where $B(\omega) = 1 + n(\omega, T)$, $\varepsilon = (\omega - \Omega)/\Gamma$, and $S = VT_p/T_e + V^2 R(\omega)$ with the Raman phonon T_p and electronic T_e matrix elements. The fitting parameters Ω and Γ (renormalized frequency and linewidth) are connected with the uncoupled Ω_0 and Γ_0 through the relations $\Omega = \Omega_0 + V^2 R(\omega)$ and $\Gamma = \Gamma_0 + V^2 \rho(\omega)$, where V is the electron-phonon coupling, and $\rho(\omega)$ and $R(\omega)$ are the imaginary and real parts of the electronic response $\chi(\omega) = -R(\omega) + i\rho(\omega)$. Five param-

eters A, Ω, Γ_0, S, and V were used as ω independent in the fitting.[24] A similar formula for the expression of the Raman efficiency was proposed in Ref. 25.

To consider orthorhombisity of the $YBa_2C_3O_{7-x}$ structure, we have to introduce polarization-dependent parameters. With this aim we assume $\Gamma=\Gamma_0+\alpha V_x^2\rho_x+\beta V_y^2\rho_y$, and in the first approximation we chose $\alpha=\beta=1$, that is, $\Gamma=\Gamma_0+V_x^2\rho_x+V_y^2\rho_y$. Then we obtain, for selected polarization ($i=xx$, or yy),

$$F_i(\omega)=\frac{A_i}{V_i^2}B(\omega)V_i^2\rho_i(\omega)\left\{\frac{\Gamma(\omega)-V_i^2\rho_i(\omega)}{\Gamma(\omega)}+\frac{V_i^2\rho_i(\omega)}{\Gamma(\omega)}\frac{\left[\frac{S_i}{V_i^2\rho_i(\omega)}+\varepsilon\right]^2}{1+\varepsilon^2}\right\}. \tag{3}$$

For $\varepsilon\gg\{1 \text{ and } S_i/[V_i^2\rho_i(\omega)]\}$, the parentheses are close to unity and, therefore, $F_i(\omega)=A_iB(\omega)\rho_i(\omega)$. It has been pointed out in Ref. 26 that the coupling constant V in Eq. (3) is combined with $\rho(\omega)$ and therefore cannot be chosen as an independent parameter for the fitting, as in Ref. 24.

By introducing a dimensionless function $g_i(\omega)=V_i^2\rho_i(\omega)/\Gamma_0$, we obtain

$$F_i(\omega)=A_i'B(\omega)g_i(\omega)\left\{1+\frac{g_i(\omega)}{1+g(\omega)}\times\left(\frac{\left[S_i\frac{1+g(\omega)}{g_i(\omega)}+(\omega-\Omega)\right]^2}{\Gamma_0^2[1+g(\omega)]^2+(\omega-\Omega)^2}-1\right)\right\}, \tag{4}$$

where $A_i'=A_i\Gamma_0/V_i^2$ and $g(\omega)=g_x(\omega)+g_y(\omega)$. Here $g_i(\omega)$ is a smooth function describing the background, and it can be used in the iteration procedure where A_i', Ω, Γ_0, and S_i are four ω-independent fitting parameters. The final formula includes five other phonon lines (at 120, 150, 430, 500, and 600 cm^{-1}), which are assumed to be Lorentzians:

$$I_i(\omega)=F_i(\omega)+\sum_{j=1}^{5}A_j\frac{\Gamma_j}{\Gamma_j^2+(\omega-\Omega_j)^2}. \tag{5}$$

Several different formulas were examined for $g(\omega)$, and the best fitting was obtained with the following formula:

$$g(\omega)=C_0+\frac{C_1\omega+C_2\omega^2}{\Gamma_e^2+(\omega-D)^2} \quad \text{at } T<T_c, \tag{6a}$$

$$g(\omega)=C_0'+C_1'\omega+C_2'\omega^2 \quad \text{at } T>T_c. \tag{6b}$$

As can be seen in Fig. 4, the fitting result is good. The temperature dependences of Ω, Γ_0, and S_i for the 340 cm^{-1} line are plotted in Fig. 5. For the OverD samples, the renormalized frequency Ω exhibits a steplike softening between 70 and 40 K. At temperatures below 40 K, the frequency is still temperature dependent. The frequency is less sensitive to temperature in the vicinity of T_c, but does not show any hardening. In the SlOverD sample, the softening occurs just below T_c and is almost saturated at temperatures below 50 K. The total softening of about 6 cm^{-1} is almost common in the OverD, SlOverD, and OptD samples. In UndD samples, the softening is very small, being about 1 cm^{-1}.

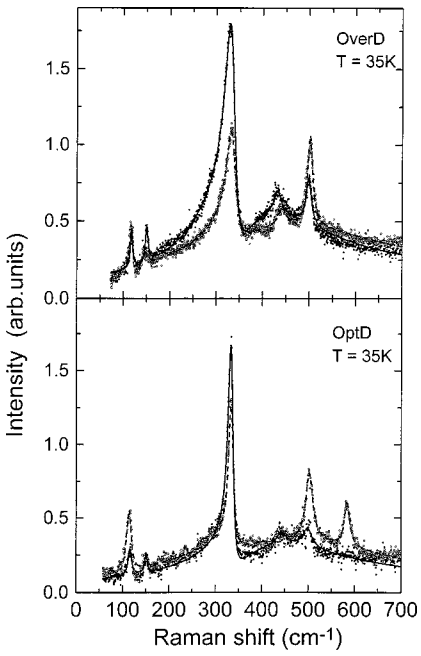

FIG. 4. The Raman spectra for the OverD and OptD twin-free $YBa_2Cu_3O_{7-x}$ single crystals at $T=35$ K. The xx polarization is shown by solid circles, and the yy polarization is shown open circles. The solid curve for xx polarization and dashed curve for yy polarization are the results of the Green fitting procedure using Eq. (5).

The uncoupled linewidth $\Gamma_0(T)$ shows smooth temperature dependence, without any anomaly below T_c. As shown by the solid curves in Fig. 5(b), this temperature dependence can be well described by a simple two-phonon-decay channel,[22] based on the Klemens-Hart model:[27,28]

$$\Gamma_0(T)=\Gamma_S+\Gamma(0)[1+2n(\omega/2,T)],$$
$$n(\omega,T)=1/[\exp(\hbar\omega/k_BT)-1], \tag{7}$$

where temperature-independent term Γ_S mainly results from phonon scattering by impurities.

The renormalized damping at the relevant phonon frequency, $\Gamma=\Gamma_0+V_x^2\rho_x+V_y^2\rho_y=\Gamma_0[1+g_x(\omega)+g_y(\omega)]$, which involves the electronic response, shows a bump at temperatures below T_c. For OverD, SlOverD, and OptD crystals, Γ has a maximum at $T^*\approx 55$, 80, and 80 K, respectively [Fig. 5(b)], where a rapid softening of the frequency just occurs [Fig. 5(a)]. The maximum of the Γ bump height decreases with reducing doping level. The superconductivity-induced effect also manifests itself in the parameter S, as shown in Fig. 5(c).

To extract the phonon parameters from the RSS, the Fano fitting approach has been widely used. Although there is a problem in the manner of subtracting the electronic background, in most cases this approach could give proper results. Of course, one has to introduce an appropriate background function and correctly pick up the meaning of the obtained results. Here we also analyze our spectra by using

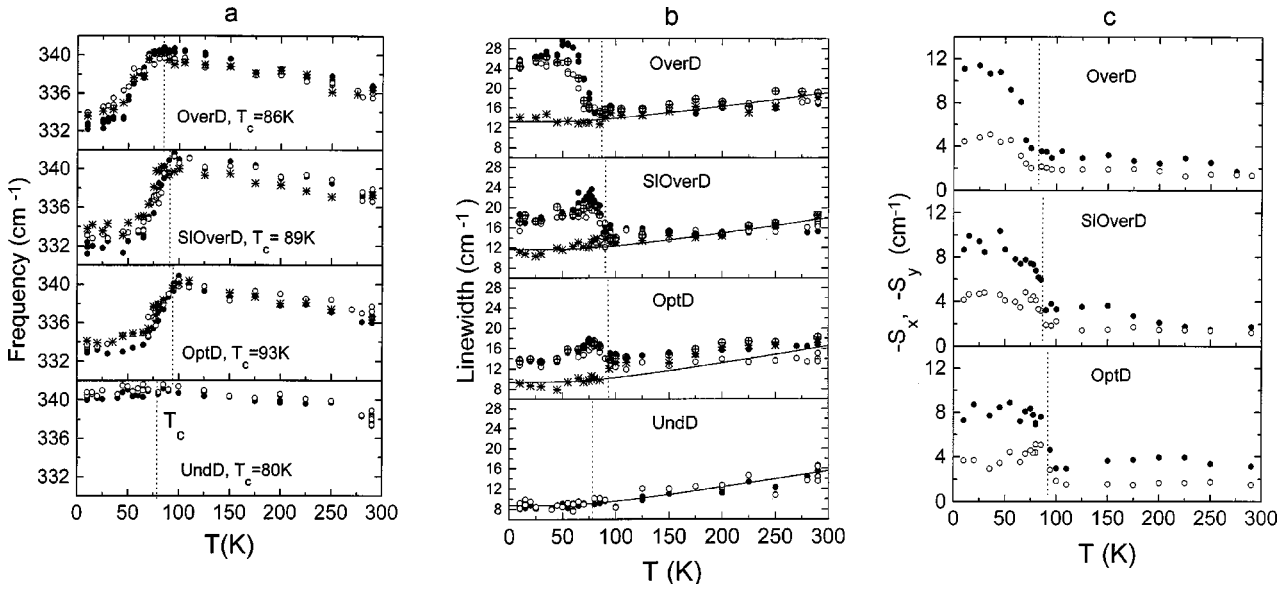

FIG. 5. Temperature dependences of the fitting parameters of the 340 cm^{-1} phonon line for the OverD, SlOverD, OptD, and UndD twin-free $YBa_2Cu_3O_{7-x}$ single crystals. (a) Renormalized frequencies $\Omega=\Omega_0+V^2R$ obtained using the FFP treatment (solid circles for the *xx* polarization and open circles for the *yy* polarization) and Green treatment (stars). (b) Renormalized linewidths $2\Gamma=2(\Gamma_0+V^2\rho)$ obtained from the FFP treatment (solid circles for the *xx* polarization and open circles for the *yy* polarization), bare linewidth $2\Gamma_0$ obtained from the Green treatment (stars) and renormalized linewidth $2\Gamma=2\Gamma_0(1+g_x+g_y)$ obtained from the Green treatment (centered circles). All lines are the results of calculations within a framework of a two-phonon-decay anharmonicity using Eq. (7). (c) *S* parameters obtained from the Green treatment (solid circles for the *xx* polarization, open circles for the *yy* polarization).

the Fano formula. We fit the RSS in the spectral region between 175 and 400 cm^{-1} using the following formula:

$$I=F(\omega)+I_0(\omega). \tag{8}$$

The first term describes the conventional Fano profile of the 340 cm^{-1} line:

$$F(\omega)=\rho(\omega)T_e^2(q+\varepsilon)^2/(1+\varepsilon^2), \tag{9}$$

where $q=(VT_p/T_e+V^2R)/\Gamma$ is so-called Fano parameter. The second term $I_0(\omega)$ represents the noninteracting part of the electronic continuum. In the present case, we choose a simple polynomial

$$I_0(\omega)=C_0+C_1\omega+C_2\omega^2. \tag{10}$$

Markedly, the fitting parameters Ω and Γ are already renormalized by the electronic response at a certain frequency. In this analysis, all of fitting parameters are kept free [free fitting parameters (FFP)], putting no constraint on different polarizations. This should lead to the polarization-dependent parameters, owing to the anisotropic electronic response.

The resultant parameters are also plotted in Fig. 5. Both for Ω and Γ, we can see good agreement of the results obtained by the two approaches. The main difference is the *x*-*y* anisotropy observed in Ω and Γ for the FFP analysis. As mentioned above, this is caused by the *x*-*y* anisotropy in the electronic response $\chi(\omega)=-R(\omega)+i\rho(\omega)$. In the Green function analysis, this anisotropy manifests itself in the parameter S_i and the $\rho_i(\omega)$ [or $g_i(\omega)$] functions, as shown in Figs. 5(c) and 6.

After confirming this consistency between the two approaches, we analyzed the RSS for the UndD crystal by the FFP fitting. As expected from the raw data, there is no distinct superconductivity-induced effect seen in the phonon parameters. Only in the frequency is a weak softening observed below T_c.

IV. DISCUSSION

Among the five A_{1g} phonon modes, the 340 cm^{-1} mode shows the most clear effect of a superconducting transition, which survives even in the UndD crystal. Considering the B_{1g}-like character of this mode, the strong phonon self-energy effect due to an electron-phonon interaction is indicative of the same B_{1g} character of the counter part, namely, a *d*-wave gap in this system.

Concerning a gap symmetry in the high-T_c superconductors, the phase sensitive experiments have given clear evidence for a *d*-wave gap.[29] The result of the electronic Raman scattering are also consistent with a *d*-wave gap.[11,30] However, there have been few reports in which the phonon Raman spectra are discussed from the viewpoint of an anisotropic gap. The phonon self-energy effects for a superconductor with the *d*-wave gap were calculated by Nicol, Jiang, and Carbotte.[10] The main difference from the case of an isotropic *s*-wave gap originates from a finite DOS below a maximum gap energy. Since the linewidth is equal to $\Gamma=\Gamma_0+V^2\rho$, a finite DOS namely, ρ below T_c, gives an additional broadening of phonons with energies smaller than the gap energy. In the present results, the linewidth behavior for the 340 cm^{-1} mode strongly supports a gap with nodes. As seen in Fig. 5(b), with lowering the temperature below T_c, the renormalized Γ is enhanced and shows a maximum at an intermediate temperature $T^*<T_c$ when a softening of this mode starts. Even below T^*, this additional broadening does not disappear and remains finite at the lowest temperature ($\sim$10 K). This is a direct indication of the remaining

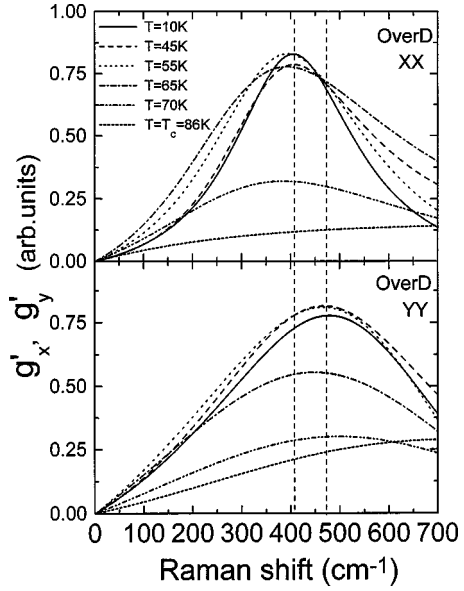

FIG. 6. The $g'(\omega)$ functions for the OverD crystal for the *xx* and *yy* polarizations at different temperatures below T_c [$g'(\omega) = g(\omega) - C_0$].

DOS around 340 cm^{-1}, which is characteristic of a gap with nodes. This cannot be expected for the isotropic *s*-wave superconductor, where the DOS below $2\Delta(T)$ is zero and thus gives no broadening of the phonon lines with $\hbar\Omega_0 < 2\Delta(0)$.

One can see more directly the gap feature with nodes in the electronic response $\rho(\omega) = g(\omega)(\Gamma_0/V^2)$ in Fig. 6. As the temperature is lowered, $\rho(\omega)$ changes from a monotonically increasing function above T_c to a peak with a long tail towards zero frequency below T_c. At high temperature near T_c, $\rho(\omega)$ is very broad.

In Fig. 7, the spectral change in $\rho(\omega)$ is represented in terms of the parameters D and Γ_e in Eq. (6a). One can find that a rapid narrowing of $\rho(\omega)$ takes place in the temperature

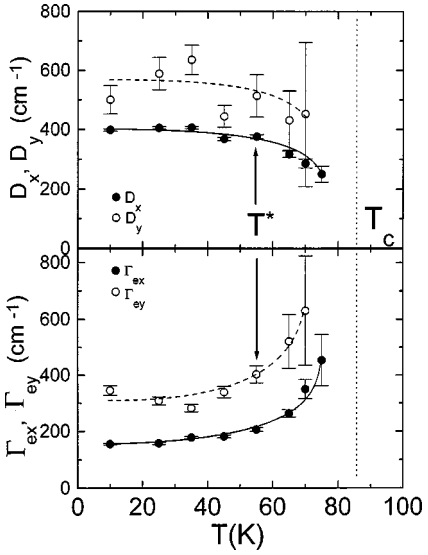

FIG. 7. Temperature dependences of D and Γ_e fitting parameters of the function $\rho(\omega) \sim g(\omega)$ for the OverD $YBa_2Cu_3O_{7-x}$ single crystals.

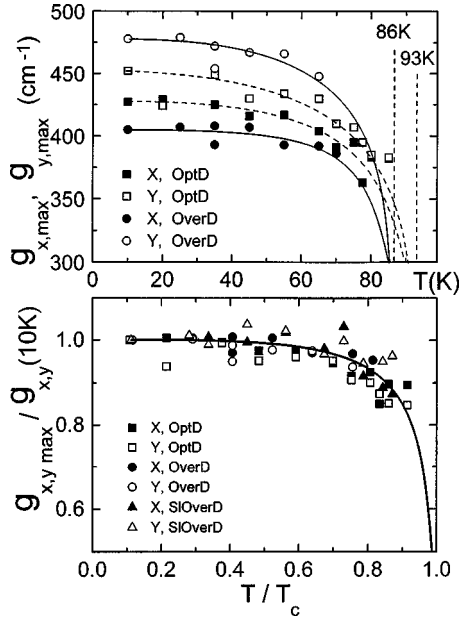

FIG. 8. Upper panel: the temperature dependences of the maximums of the $g(\omega)$ functions for the *xx* and *yy* polarizations for the OverD and OptD twin-free $YBa_2Cu_3O_{7-x}$ crystals. Lower panel: normalized temperature dependence $g_{max}(T/T_c)/g(T=10\,K)$ for OverD, SlOverD, and OptD crystals.

region $T^* < T < T_c$ (T^* is about 50 K for the OverD crystal). The temperature dependence of Γ for the 340 cm^{-1} line is attributed to the temperature dependence of the ρ value at 340 cm^{-1}, which is predominantly governed by this strong change in the width of $\rho(\omega)$. It is different from the picture, assumed in the Nicol-Jiang-Crbotte model, in which with decreasing T the $\rho(\omega)$ peak shifts from $\omega = 0$ to higher frequency and crosses the phonon frequency (340 cm^{-1}) at $T = T_g$, keeping a sharp peak profile of $\rho(\omega)$.

An abrupt narrowing at $T^* < T < T_c$ and an almost T-insensitive peak frequency of $\rho(\omega)$ below T^* are commonly observed in all the crystals for both *xx* and *yy* spectra. As is seen in Fig. 8, the temperature dependence of $\rho_{max} \sim g_{max}$ can be scaled as a function of normalized temperature T/T_c. The frequency of the $\rho(\omega)$ peak, which can be resolved only below a certain temperature ($< T_c$), is almost T independent. The abrupt appearance of a large gap instead of a gradual gap growth with reducing T is also observed in the tunneling spectroscopy[31] and in the electronic Raman spectra of $Bi_2Sr_2CaCu_2O_z$.[32] This might be related to an opening of the pseudogap above T_c.

As to the doping dependence of the gap, with reducing oxygen content all superconductivity-induced effects on the 340 cm^{-1} line become weak. One simple scenario is that it is due to an increase in the gap energy. The other possible origin is that the whole electronic response including its enhancement near the gap energy dramatically decreases when the system goes to underdoping. Figure 9 shows the doping dependence of $\rho(\omega) \sim g(\omega)$ at 10 K for *xx* and *yy* spectra. As doping is reduced, the peak intensity of $\rho(\omega)$ decreases and the peak width increases. These spectral changes in $\rho(\omega)$ can explain the change in the magnitude of residual Γ at 10 K, which scales with ρ at $\omega = 340\,cm^{-1}$. Such a change in the electronic spectrum in the superconducting state is consistent

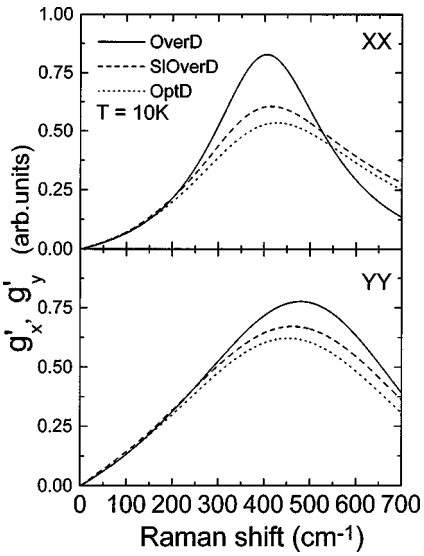

FIG. 9. The $g'(\omega)$ functions for OverD, SlOverD, and OptD crystals for the *xx* and *yy* polarizations at $T=10\,\mathrm{K}$ $[g'(\omega)=g(\omega)-C_0]$.

with the specific heat results in $YBa_2Cu_3O_{7-x}$.[33] The specific heat jump at T_c becomes broad when the oxygen content decreases, suggesting the nature of this phase transition, i.e., the superconducting transition, changes with reducing a doping level.

Finally, we discuss the *x-y* anisotropy in the superconductivity-induced effects on the RSS. As we reported in our previous paper,[12] a pronounced *x-y* difference in the RSS is observed in the OverD sample. In this paper we showed a similar effect also for the SlOverD and OptD samples. In the Green function analysis, *x-y* anisotropy appears in S and $g(\omega)$. The origin of anisotropy in $S=VT_p/T_e+V^2R(\omega)$ is supposed to be the anisotropy in both $R(\omega)$ and VT_p/T_e. However, considering the less temperature-sensitive nature of T_p/T_e, a remarkable enhancement of the *x-y* anisotropy of S below T_c [Fig. 5(b)] must be caused mainly by the anisotropy in $R(\omega)$ below T_c. On the other hand, the anisotropy in $\rho(\omega)$ is directly seen in Fig. 6. Therefore, the electronic response $\chi(\omega)=-R(\omega)+i\rho(\omega)$ is anisotropic, as we claimed in Refs. 12 and 34 by analyzing the RSS by the FFP fitting.[35]

In the $\rho(\omega)$ function, we can see two features related to the *x-y* anisotropy. The first is the difference of the maximum of $\rho(\omega)$ in the *xx* and *yy* polarizations, and the second is the difference in the peak width of $\rho(\omega)$. The former is represented as the parameter D in Eq. (6a), while the latter is as Γ_e. The temperature dependence of these parameters is shown in Fig. 7 for the OverD crystals. The *x-y* splitting of the maximums of the electronic response functions $\rho_{\max}$ (Figs. 8 and 9) suggests a difference in the gap amplitude $\Delta(\mathbf{k},T=0)$ between the $\mathbf{k}_x$ and $\mathbf{k}_y$ directions in the Brillouin zone. At $T=10\,\mathrm{K}$, the splitting is estimated at about 75 cm^{-1} in OverD, about 50 cm^{-1} in SlOverD, and about 25 cm^{-1} in OptD samples.

The width of the $\rho(\omega)$ peak is also different in the *xx* and *yy* polarizations. For OverD crystals at low temperature (10–50 K), the Γ_e parameter is about 300 cm^{-1} in the *yy* polarization and about 150 cm^{-1} in the *xx* polarization (Fig. 7). In the RSS of the SlOverD and OptD samples, the 2Δ peak in the electronic background broadens and the Γ_e parameter is estimated to be about 350–400 cm^{-1} in the *yy* polarization and about 200–250 cm^{-1} in the *xx* one. With increasing temperature, the intensity of the $\rho(\omega)$ maximum decreases and its profile becomes broader (Γ_e increases), and eventually transforms into a background well described by the formula $C_0'+C_1'\omega+C_2'\omega^2$, which was used for fitting at $T>T_c$ in Eq. (6b).

A possible origin of the *x-y* anisotropy in the electronic response $\chi(\omega)$ is the mixture of the *d* and *s* components due to the orthorhombicity in crystal structure of $YBa_2Cu_3O_7$ or due to the contribution from the CuO chain. The gap with $d+s$ symmetry, represented as

$$\Delta_{d+s}=\Delta_d(\cos k_x-\cos k_y)+\Delta_s(\cos k_x+\cos k_y), \quad (11)$$

was theoretically predicted for orthorhombic structures.[37] However, we have to notice that the observed *x-y* anisotropy is rapidly weakened with reducing oxygen content within a very narrow doping range. The orthorhombicity of the $YBa_2Cu_3O_{7-x}$ crystals is not strongly suppressed with such a small change in the oxygen content.[38] Therefore, an alternative source of the *s*-wave contribution is required.

One simple scenario is the mixing of the chain electronic response via the off-diagonal term in the Raman vertex. If the CuO chain has an independent superconductivity channel with anisotropic *s*-wave symmetry, an admixture of this *s* component with the *d*-wave gap in the CuO_2 plane can give the *x-y* anisotropy described in Eq. (11). Since superconductivity in the chain is seriously affected by a small amount of oxygen content, it is likely that the *x-y* anisotropy due to the contribution of the chain superconductivity decreases radically with reducing oxygen content.

Another possibility is the admixture of the anisotropic *s*-wave component in the CuO_2 plane. Only in the orthorhombic structure with *x-y*-anisotropic effective mass, adding a lifetime broadening of the gap peak, can one obtain the *x-y* anisotropy in $\rho(\omega)$. If the *s* component increases with doping, the observed development of *x-y* anisotropy can be explained.

V. CONCLUSIONS

In this paper, precise temperature and polarization dependences of RSS have been investigated for twin-free $YBa_2Cu_3O_{7-x}$ single crystals with four compositions, from overdoped to slightly underdoped composition. Clear out-of-plane and/or in-plane anisotropies of RSS have been observed at all temperatures. In an attempt to describe the entire picture of the RSS in $YBa_2Cu_3O_{7-x}$, one can expect that there is a mixing of different anisotropy effects, which are connected with the electron-phonon interaction, Raman vertex, and superconducting gap.

The main features of the observed superconductivity-induced effects on the 340 cm^{-1} line, such as a maximum of the line broadening accompanied by a steplike softening at a certain temperature T^* and the remaining superconductivity-induced broadening at 10 K, are well described within the model for an anisotropic gap. Only by a small change in oxygen content do all the superconductivity-induced effects diminish rapidly. This suggests a drastic change in the super-

conducting gap nature, which is also seen in the extracted electronic response function $\rho(\omega)$ as the broadening and weakening of a gap feature in the oxygen-deficient crystals. This qualitative change of the gap is consistent with the results of the other experiments such as the specific heat.

The *x-y* anisotropy in superconductivity-induced effects was observed not only in the OverD sample, but also in the SlOverD and OptD samples. This *x-y* anisotropy was successfully described by the anisotropy in S and $\rho(\omega)$, in the Green function analysis, which is predominantly attributed to the anisotropic electronic response $\chi(\omega) = -R(\omega) + i\rho(\omega)$. This anisotropy was found to be strongly suppressed with reducing oxygen content, owing either to a reduction of the contribution from the superconductivity in the CuO chain or to a decrease of the *s*-wave component induced in the CuO_2 plane.

ACKNOWLEDGMENTS

The authors are deeply thankful to A. G. Panfilov for numerous helpful discussions. This work was supported by New Energy and Industrial Technology Development Organization (NEDO) as Collaborative Research and Development of Fundamental Technologies for Superconductivity Applications.

*Permanent address: A. F. Ioffe Physical-Technical Institute, 194021 St. Petersburg, Russia.

[1] R. M. Macfarlane, H. J. Rosen, and H. Seki, Solid State Commun. **63**, 831 (1987).
[2] A. Wittlin, R. Liu, M. Cardona, L. Genzel, W. Konig, W. Bauhofer, H. Mattausch, A. Simon, and F. Garcia-Alvarado, Solid State Commun. **64**, 477 (1987).
[3] S. L. Copper, F. Slakey, M. V. Klein, J. P. Rice, E. D. Bukowski, and D. M. Ginsberg, Phys. Rev. B **38**, 11 934 (1988).
[4] E. Altendorf, X. K. Chen, J. C. Irwin, R. Liang, and W. N. Hardy, Phys. Rev. B **47**, 8140 (1993).
[5] B. Friedl, C. Thomsen, and M. Cardona, Phys. Rev. Lett. **65**, 915 (1990).
[6] C. Thomsen, M. Cardona, B. Friedl, C. O. Rodriguez, I. I. Mazin, and O. K. Andersen, Solid State Commun. **75**, 219 (1990).
[7] E. Altendorf, J. Chrzanowski, J. C. Irwin, A. O'Reilly, and W. N. Hardy, Physica C **175**, 47 (1991).
[8] K. F. McCarty, H. B. Radousky, J. Z. Liu, and R. N. Shelton, Phys. Rev. B **43**, 13 751 (1991).
[9] R. Zeyher and G. Zwicknagl, Solid State Commun. **66**, 617 (1988); Z. Phys. B: Condens. Matter **78**, 175 (1990).
[10] E. J. Nicol, C. Jiang, and J. P. Carbotte, Phys. Rev. B **47**, 8131 (1993).
[11] T. P. Devereaux and D. Einzel, Phys. Rev. B **51**, 16 336 (1995).
[12] M. F. Limonov, A. I. Rykov, S. Tajima, and A. Yamanaka, Phys. Rev. Lett. **80**, 825 (1998).
[13] A. I. Rykov, W. J. Jang, H. Unoki, and S. Tajima, in *Advances in Superconductivity VIII*, edited by H. Hayakawa and Y. Enomoto (Springer-Verlag, Tokyo, 1996), p. 341.
[14] M. Cardona, R. Liu, C. Thomsen, M. Bauer, L. Genzel, W. Konig, and A. Wittlin, Solid State Commun. **65**, 17 (1988).
[15] M. F. Limonov and A. P. Mirgorodskii, Zh. Eksp. Teor. Fiz. **106**, 1794 (1994) [JETP **79**, 973 (1994)].
[16] V. D. Kulakovskii, O. V. Misochko, V. B. Timofeev, M. I. Eremets, E. S. Itskevich, and V. V. Struzhkin, Pis'ma Zh. Eksp. Teor. Fiz. **47**, 536 (1988) [JETP Lett. **47**, 626 (1988)].
[17] K. Syassen, M. Hanfland, K. Strossner, M. Holtz, W. Kress, M. Cardona, U. Schroder, J. Prade, A. D. Kulkarni, and F. W. de Wette, Physica C **153-155**, 264 (1988).
[18] A. I. Rykov, M. F. Limonov, and S. Tajima, in *Advances in Superconductivity IX*, edited by S. Nakajima and M. Murakami (Springer-Verlag, Tokyo, 1997), p. 391.
[19] C. Thomsen, in *Light Scattering in Solids VI*, edited by M. Cardona and G. Guntherodt (Springer-Verlag, Berlin, 1991).
[20] Yu. E. Kitaev, M. F. Limonov, A. G. Panfilov, R. A. Evarestov, and A. P. Mirgorodsky, Phys. Solid State **36**, 475 (1994).
[21] Yu. E. Kitaev, M. F. Limonov, A. P. Mirgorodsky, A. G. Panfilov, and R. A. Evarestov, Phys. Rev. B **49**, 9933 (1994).
[22] M. Balkanski, R. F. Wallis, and E. Haro, Phys. Rev. B **28**, 1928 (1983).
[23] M. V. Klein, in *Light Scattering in Solids*, edited by M. Cardona (Springer-Verlag, Heidelberg, 1991).
[24] X. K. Chen, E. Altendorf, J. C. Irwin, R. Liang, and W. N. Hardy, Phys. Rev. B **48**, 10 530 (1993).
[25] A. Bock, S. Ostertun, R. Das Sharma, M. Rübhausen, K.-O. Subke, and C. T. Rieck, Phys. Rev. B **60**, 3532 (1999).
[26] A. G. Panfilov, S. Tajima, and A. Yamanaka, in *Advances in Superconductivity XI*, edited by N. Koshizuka and S. Tajima (Springer Verlag, Tokyo, 1999), p. 77.
[27] P. G. Klemens, Phys. Rev. **148**, 845 (1966).
[28] T. R. Hart, R. L. Aggarwal, and B. Lax, Phys. Rev. B **1**, 638 (1970).
[29] D. A. Wollman, D. J. van Harlinger, W. C. Lee, D. M. Ginsberg, and A. J. Leggett, Phys. Rev. Lett. **71**, 2134 (1993).
[30] For example, see D. Einzel and R. Hackl, J. Raman Spectrosc. **27**, 307 (1996).
[31] A. Matsuda, S. Sugita, and T. Watanabe, in *Advances in Superconductivity XI* (Ref. 26), p. 151.
[32] A. Yamanaka, H. Takato, F. Minami, K. Inoue, and S. Takekawa, Physica C **185-189**, 1027 (1991).
[33] J. W. Loram, K. A. Mirza, J. R. Cooper, and W. Y. Liang, Phys. Rev. Lett. **71**, 1740 (1993).
[34] M. F. Limonov, A. I. Rykov, S. Tajima, and A. Yamanaka, Phys. Rev. Lett. **81**, 2181 (1998).
[35] Note that the authors of the Comment in Ref. 36 attempted to explain the *x-y* anisotropy in the RSS of the OverD $YBa_2Cu_3O_{7-x}$ crystals by the anisotropy in the Raman vertices T_p and T_e only, without *x-y* anisotropy in the electronic response $\chi(\omega) = -R(\omega) + i\rho(\omega)$.
[36] T. Strohm, V. I. Belitsky, V. G. Hadjiev, and M. Cardona, Phys. Rev. Lett. **81**, 2180 (1998).
[37] Q. P. Li, B. E. C. Koltenbah, and R. Joynt, Phys. Rev. B **48**, 437 (1993); C. O'Donovan and J. P. Carbotte, *ibid.* **52**, 16 208 (1995); J. Low Temp. Phys. **105**, 495 (1996); K. Maki and M. T. Beal-Monod, Phys. Lett. A **208**, 365 (1995).
[38] J. P. Jorgensen, B. W. Veal, A. P. Paulikas, L. J. Nowicki, G. W. Crabtree, H. Claus, and W. K. Kwok, Phys. Rev. B **41**, 1863 (1990).